

Deterministic Controlled-NOT gate for single-photon two-qubit quantum logic

Marco Fiorentino* and Franco N. C. Wong

Research Laboratory of Electronics, Massachusetts Institute of Technology, Cambridge, MA 02139

We demonstrate a robust implementation of a deterministic linear-optical Controlled-NOT (CNOT) gate for single-photon two-qubit quantum logic. A polarization Sagnac interferometer with an embedded 45° -oriented dove prism is used to enable the polarization control qubit to act on the momentum (spatial) target qubit of the same photon. The CNOT gate requires no active stabilization because the two spatial modes share a common path, and it is used to entangle the polarization and momentum qubits.

PACS numbers: 03.67.-a, 03.67.Lx, 42.50.Dv, 03.67.Mn

Knill, Laflamme, and Milburn [1] show that probabilistic two-qubit operations implemented in linear optical circuits with ancilla photons can be used to build a scalable quantum computer. Their work has stimulated much attention on the experimental realization of linear optics quantum computation (LOQC) protocols, and simple two-qubit gates based on quantum interference and postselection have been demonstrated [2].

It has been recognized that building a deterministic QIP is possible for systems that use several degrees of freedom of a single photon to encode multiple qubits [3]. This type of QIP cannot be used for general-purpose quantum computation because it requires resources that grow exponentially with the number of qubits. Nevertheless, there is a growing interest in few-qubit QIPs. Small deterministic QIPs have been used to demonstrate basic quantum logic protocols [4]. Several authors have suggested the use of three- or four-qubit QIP based on two degrees of freedom of a photon in combination with sources of hyperentangled photons (i.e., photons that are entangled in more than one degree of freedom) for an all-or-nothing demonstration of nonlocality [5], complete Bell's state measurements [6], and quantum cryptography [7]. Small QIPs have also been proposed as a way to implement quantum games [8]. Kim [9] has demonstrated the creation of entanglement between the polarization and momentum qubits of a single photon by introducing two possible paths for the single photon and allowing the phase and polarization for each path to be controlled separately. This method may have limited application potential due to the interferometric arrangement of the two paths.

The utility of single-photon two-qubit (SPTQ) QIP depends on one's ability to create and manipulate the individual qubits (qubit rotation) and to implement two-qubit quantum gates in a robust experimental setup. In this Letter, we demonstrate the first experimental realization of a deterministic linear optical Controlled-NOT (CNOT) gate for two-qubit photons, with the polarization serving as the control qubit and the momentum as

the target qubit. Our implementation eliminates a roadblock for SPTQ quantum logic protocols by using a simple and compact polarization Sagnac interferometer with an internal dove prism oriented at 45° that requires no stabilization of the path lengths. This SPTQ CNOT gate can be utilized to perform a variety of quantum logic operations that are necessary for SPTQ QIP implementation. In particular, we have used it to demonstrate the ease and efficiency of entangling the polarization and momentum qubits of a single photon. Finally, the SPTQ CNOT gate is especially suitable for use with entangled photon pairs for creating more complex entangled states of three or more qubits and opens the way to the implementation of SPTQ protocols for few-qubit QIP.

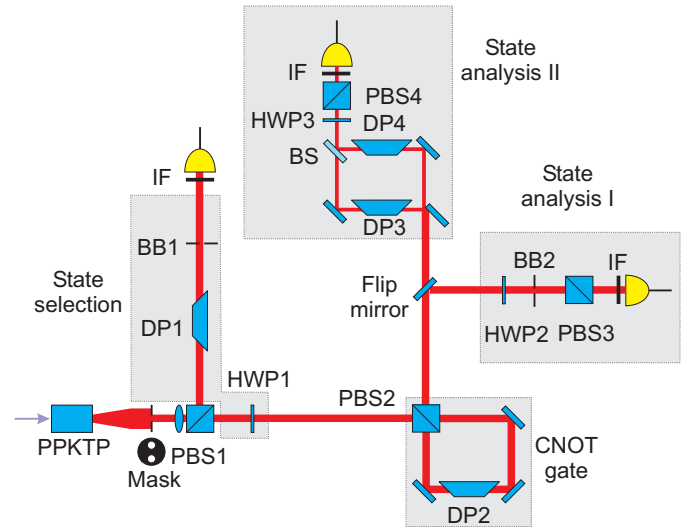


FIG. 1: Schematic of experimental setup. PPKTP: periodically poled KTP crystal. PBS: polarizing beam splitter. HWP: half-wave plate. DP: dove prism. BS: 50-50 beam splitter. BB: beam block that allows one to block the L or R part of the beam. IF: 1-nm interference filter centered at 797 nm.

As shown in Fig. 1, the CNOT gate is a polarization Sagnac interferometer containing a dove prism whose base is oriented at a 45° angle relative to the horizontal plane. This interferometer is similar to a non-polarizing Sagnac interferometer for measuring the spatial Wigner

*Electronic address: mfiore@mit.edu

function [10]. The input polarizing beam splitter (PBS2) directs horizontally (vertically) polarized input light to travel in a clockwise (counterclockwise) direction. As viewed by each beam, the dove prism orientation is different for the two counter-propagating beams such that the transformation of the input spatial image differs for the horizontal (H) and vertical (V) polarizations. Specifically, the top-bottom (T - B) sections of the input beam are mapped onto the right-left (R - L) sections of the output beam for H -polarized light but onto the L - R sections for V -polarized light. If we identify $|H\rangle$, $|T\rangle$, and $|R\rangle$ with the logical $|0\rangle$ and $|V\rangle$, $|B\rangle$, and $|L\rangle$ with the logical $|1\rangle$, this setup implements a polarization-controlled NOT (P-CNOT) gate in which the polarization is the control qubit and the momentum (or spatial) mode is the target qubit. A key advantage of the Sagnac interferometer is that the same amount of phase delay is added to the two counterpropagating beams, thus removing the need for active control of the interferometer. We should point out that the complementary momentum-controlled NOT (M-CNOT) gate in which the momentum is the control qubit and the polarization is the target qubit can be realized with a half-wave plate (HWP) oriented at 45° relative to the horizontal position and inserted in the path of the B beam. It can also be shown [12] that it is possible, using linear optical components, to perform arbitrary qubit rotation on either the polarization or momentum qubit without disturbing the state of the other qubit of a single photon.

Figure 1 shows the experimental setup for demonstrating the CNOT gate operation. A 10-mm-long periodically poled hydrothermally grown potassium titanyl phosphate (KTP) crystal (9.0- μm grating period) was continuous-wave (cw) pumped at 398.5 nm for type-II collinear frequency-degenerate parametric down-conversion [13]. We have previously obtained a signal-idler quantum interference visibility of 99% for this source. The idler-triggered signal beam was used as a single-photon source for the input to the CNOT gate. The orthogonally polarized signal and idler photons were separated by PBS1 in Fig. 1, and the signal polarization could be rotated by HWP1. We used postselection to set the signal momentum (T or B). We first had to verify that the down-converted photon pairs show correlation in momentum (T - B). To do this we collimated the down-converted photons and sent them through a mask with two apertures (1.5 mm diameter, 2.5 mm center-to-center distance) that defined the top and bottom beams. After the PBS1 the H -polarized signal and V -polarized idler were separated, spectrally filtered with a 1-nm interference filter (IF) centered at 797 nm, and detected by two Si photon-counting modules (Perkin Elmer SPCM-AQR-14). Signal-idler coincidence counts were measured with a fast AND gate based on positive emitter coupled logic (PECL) with a coincidence window of ~ 1 ns [11]. The 1-ns coincidence window and singles count rates of less than $10^5/\text{s}$ ensure negligible accidental coincidence counts. When we blocked the top (bottom) idler beam

after PBS1 to pass the bottom (top) idler photons, only the top (bottom) signal beam yielded coincidences, thus establishing the momentum correlation between the signal and idler photons. We used the same collimation and mask setup for the input to the CNOT gate. By blocking either the T or B section of the idler with the beam blocker (BB1), we were able to postselect the momentum state of the signal photon to be T or B , respectively.

Momentum entanglement [14] in spontaneous parametric down-conversion is the basis for the generation of polarization entanglement from a noncollinearly phase-matched down-conversion crystal by use of overlapping cones of emitted photons [15]. One can therefore take advantage of the natural momentum entanglement of down-converted photon pairs to generate more complex entangled states. The state of a pair of down-converted photons is:

$$|\Theta\rangle = \frac{1}{\sqrt{2}} (|0110\rangle + |0011\rangle), \quad (1)$$

where the four qubits are written in the form of $|P_S M_S P_I M_I\rangle$ for the polarization (P) and momentum (M) qubits of the signal (S) and idler (I) photons. Applying SPTQ quantum logic to a pair of entangled photons presents some interesting possibilities. For example, a swap operation can be realized with a sequence of three CNOT gates. If we apply the swap operation (a P-CNOT gate, followed by a M-CNOT gate and another P-CNOT gate) to both photons of $|\Theta\rangle$, we transform the momentum-entangled state to a polarization-entangled state

$$|\Theta\rangle_{\text{swap}} = \frac{1}{\sqrt{2}} (|1001\rangle + |0011\rangle). \quad (2)$$

Another example is the application of a single M-CNOT gate to both signal and idler photons to obtain the four-qubit Greenberger-Horne-Zeilinger (GHZ) state

$$|\Theta\rangle_{\text{GHZ}} = \frac{1}{\sqrt{2}} (|1110\rangle + |0001\rangle). \quad (3)$$

We characterized the CNOT gate by injecting in turn each of the four natural basis states of the SPTQ $|PM\rangle$ basis and analyzing the output state by means of BB2 and HWP2. Single-photon input is guaranteed by signal-idler coincidence counting. We note that for the PBS used in the CNOT gate setup, the H -polarized light suffered a $\sim 10\%$ transmission loss ($\sim 5\%$ per passage through PBS2). This imbalance was corrected by inserting inside the Sagnac interferometer a thin glass plate near the Brewster angle for the horizontal polarization and rotating it to introduce an appropriate amount of differential loss between the two polarizations. Figure 2 displays the measured truth table of the CNOT gate, showing clearly the expected behavior of the gate. For each input state the probability sum of the erroneous outcomes is only $\sim 1\%$. There is a slight asymmetry between the H - and V -polarized outputs because the thin-plate compensation was not perfect. The table of truth

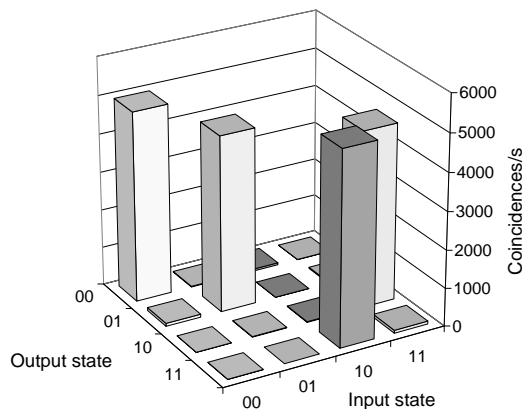


FIG. 2: Coincidence count rates as a function of the projected output state for a given input state.

we measured is a necessary consequence but not a sufficient proof that the device is a CNOT gate, whose complete characterization requires quantum process tomography [16] that is experimentally challenging and time consuming. However, as an indirect proof of its CNOT functionality, it is adequate to demonstrate that the gate preserves quantum coherence and creates entanglement.

It is well known that a CNOT gate can be used to entangle two qubits. Indeed for an input product state

$$|\Psi\rangle_{IN} = \frac{1}{\sqrt{2}}(|0\rangle_C + |1\rangle_C) \otimes |0\rangle_T, \quad (4)$$

where the subscripts C and T refer to the control (polarization) and target (momentum) qubits, respectively, the CNOT-gate output is the entangled state

$$|\Psi\rangle_{OUT} = \frac{1}{\sqrt{2}}(|0\rangle_C|0\rangle_T + |1\rangle_C|1\rangle_T). \quad (5)$$

To create the input state $|\Psi\rangle_{IN}$ HWP1 was set to rotate the signal polarization by 45° and the T -path of the idler beam was blocked, thus generating the desired state $|\Psi\rangle_{IN}$ by post selection. For the output state analysis, we used BB2, HWP2, and PBS3 (state analysis I in Fig. 1) to project the output onto

$$|\Psi\rangle_1 = [\cos\theta_A|0\rangle_C + \sin\theta_A|1\rangle_C] \otimes |0\rangle_T, \quad (6)$$

$$|\Psi\rangle_2 = [\cos\theta_A|0\rangle_C + \sin\theta_A|1\rangle_C] \otimes |1\rangle_T, \quad (7)$$

where θ_A is polarization analysis angle (equal to twice the angle setting) of HWP2. We measured the projected output as a function of θ_A and obtained the expected curves of the signal-idler coincidence counts shown in Fig. 3. The fits show a visibility of $98 \pm 1\%$ for $|\Psi\rangle_1$ and $96.2 \pm 0.8\%$ for $|\Psi\rangle_2$. These measurements alone, however, do not imply that the output state is entangled, as a mixture of the two states $|0\rangle_C|0\rangle_T$ and $|1\rangle_C|1\rangle_T$ would yield the same projective results.

Similar to a test of two-photon polarization entanglement, it is necessary to make a projective measurement

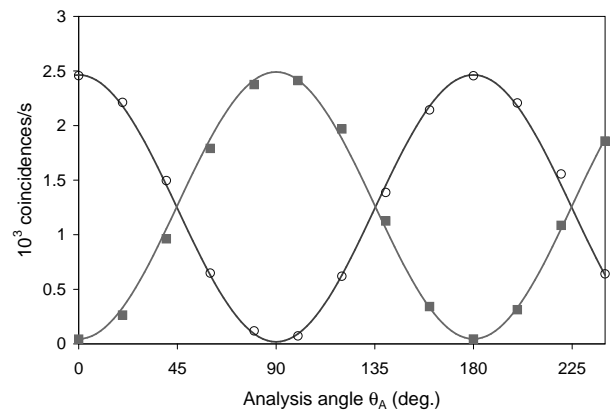


FIG. 3: Characterization of the entangled state $|\Psi\rangle_{OUT}$ by projecting it onto $|\Psi\rangle_1$ (circles) and $|\Psi\rangle_2$ (squares) versus analysis angle θ_A . The lines are fits to the data.

along $|0\rangle \pm |1\rangle$ in the momentum space with states such as

$$|\Psi\rangle_3 = [\cos\theta_A|0\rangle_C + \sin\theta_A|1\rangle_C] \otimes \frac{(|0\rangle_T + |1\rangle_T)}{\sqrt{2}}, \quad (8)$$

$$|\Psi\rangle_4 = [\cos\theta_A|0\rangle_C + \sin\theta_A|1\rangle_C] \otimes \frac{(|0\rangle_T - |1\rangle_T)}{\sqrt{2}} \quad (9)$$

and verify that the coincidences follow the expected curves. To project the output state $|\Psi\rangle_{OUT}$ onto $|\Psi\rangle_3$ and $|\Psi\rangle_4$ we used the state analysis setup II shown in Fig. 1. This was an interferometer for overlapping the L and R output beams of the CNOT gate at a 50-50 beam splitter. The two arms of the interferometer must be matched to within a coherence length of the down-converted photons, which, in our case, was determined by the 1-nm IF placed in front of the detector. Two dove prisms, one that flipped the beam vertically and the other horizontally, were placed in the interferometer arms to obtain the proper orientation for the spatial overlap of the CNOT L and R outputs. By scanning the length of one arm of the interferometer and passing the photons through HWP3 and PBS4 the state was projected onto

$$|\Psi\rangle_\phi = [\cos\theta_A|0\rangle_C + \sin\theta_A|1\rangle_C] \otimes \frac{(|0\rangle_T + e^{i\phi}|1\rangle_T)}{\sqrt{2}}, \quad (10)$$

where the phase ϕ is determined by the path length difference between the two arms of the interferometer and θ_A is the polarization analysis angle. For $\phi = 0$ and $\phi = \pi$ we obtain states $|\Psi\rangle_3$ and $|\Psi\rangle_4$, respectively. In the measurements we recorded the detected coincidences while scanning the length of one interferometer arm for different settings of the polarization analyzer (see inset of Fig. 4 for one of such traces). For each θ_A the data points are fitted with the curve $\alpha + \beta \sin^2(\delta t + \gamma)$ where α , β , δ , and γ are fit parameters and t is the scan time. The fitted maxima and minima are plotted in Fig. 4. The fitted curves in Fig. 4 yield a visibility of $90.8 \pm 0.8\%$ for $|\Psi\rangle_3$ and $91.7 \pm 1.6\%$ for $|\Psi\rangle_4$, indicating an excellent

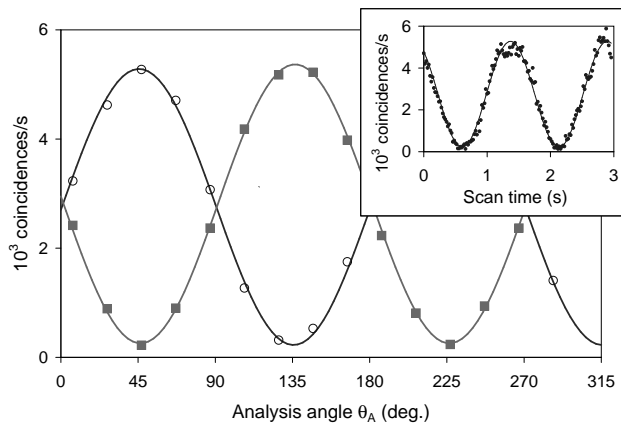


FIG. 4: Characterization of the entangled state $|\Psi\rangle_{OUT}$ by projecting it onto $|\Psi\rangle_3$ (circles) and $|\Psi\rangle_4$ (squares) for different analysis angles θ_A . The lines are fits to the data. A pump power higher than that used for Fig. 3 accounts for the higher coincidence counts. Inset: raw data for an interferometer scan with $\theta_A = 25^\circ$; the line is a fit to the data.

entangling capability of the CNOT gate. The curves are shifted by about 1° with respect to the expected value

of 45° . We attribute this shift to an imbalance in the interferometer due to a deviation of the beam splitter reflectivity from 50%.

In conclusion we have presented an implementation of a deterministic CNOT gate that uses the polarization and momentum degrees of freedom of a single photon as the control and target qubits, respectively. Based on a polarization Sagnac interferometer with an embedded dove prism, the gate is built with linear optical components, is robust and does not require any active stabilization. This device, in conjunction with sources of entangled photons, can be utilized to create the four-qubit GHZ state, to investigate nonstatistical violation of Bell's inequality [5], and for efficient two-photon Bell's state analysis [6]. We believe these more complex entanglement sources together with single-photon two-qubit quantum logic can be used to perform special computational tasks in a variety of few-qubits quantum computing and quantum communication protocols.

The authors would like to acknowledge K. Banaszek and V. Giovannetti for useful discussion. This work was supported by the DoD Multidisciplinary University Research Initiative (MURI) program administered by the Army Research Office under Grant DAAD-19-00-1-0177.

-
- [1] E. Knill, R. Laflamme, and G. J. Milburn, *Nature* **409**, 46 (2001).
 - [2] T. B. Pittman, B. C. Jacobs, and J. D. Franson, *Phys. Rev. Lett.* **88**, 257902 (2002); *Phys. Rev. A* **66**, 052305 (2002); T. B. Pittman, M. J. Fitch, B. C. Jacobs, and J. D. Franson, *Phys. Rev. A* **68**, 032316 (2003)
 - [3] N. J. Cerf, C. Adami, and P. G. Kwiat, *Phys. Rev. A* **57**, R1477 (1998); J. C. Howell and J. A. Yeazell, *Phys. Rev. A* **61**, 052303 (2000); B.-G. Englert, C. Kurtsiefer, and H. Weinfurter, *Phys. Rev. A* **63**, 032303 (2001).
 - [4] P. G. Kwiat, J. R. Mitchell, P. D. D. Schwindt, and A. G. White, *J. Mod. Opt.* **47**, 257 (2000); Y. Mitsumori, J. A. Vaccaro, S. M. Barnett, E. Andersson, A. Hasegawa, M. Takeoka, and M. Sasaki, *Phys. Rev. Lett.* **91**, 217902 (2003).
 - [5] Z.-B. Chen, J.-W. Pan, Y.-D. Zhang, C. Brukner, and A. Zeilinger, *Phys. Rev. Lett.* **90**, 160408 (2003).
 - [6] S. P. Walborn, S. Pádua, and C. H. Monken, *Phys. Rev. A* **68**, 042313 (2003).
 - [7] M. Genovese and C. Novero, *Eur. Phys. J. D* **21**, 109 (2002).
 - [8] K.-Y. Chen, T. Hogg, and R. Beausoleil, *quant-ph/0301013*.
 - [9] Y.-H. Kim, *Phys. Rev. A* **67**, 040301(R) (2003).
 - [10] E. Mukamel, K. Banaszek, I. A. Walmsley, and C. Dorrer, *Opt. Lett.* **28**, 1317 (2003).
 - [11] T. Kim, M. Fiorentino, P. V. Gorelik, and F. N. C. Wong, (submitted to *Rev. Sci. Instrum.*)
 - [12] F. N. C. Wong and M. Fiorentino (unpublished).
 - [13] C. E. Kuklewicz, M. Fiorentino, G. Messin, F. N. C. Wong, and J. H. Shapiro, *Phys. Rev. A* **69**, 013807 (2004); M. Fiorentino, G. Messin, C. E. Kuklewicz, F. N. C. Wong, and J. H. Shapiro, *Phys. Rev. A* **69**, 041801(R) (2004).
 - [14] J. G. Rarity and P. R. Tapster *Phys. Rev. Lett.* **64**, 2495 (1990).
 - [15] P. G. Kwiat, K. Mattle, H. Weinfurter, A. Zeilinger, A. V. Sergienko, and Y. Shih, *Phys. Rev. Lett.* **75**, 4337 (1995).
 - [16] J. F. Poyatos, J. I. Cirac, and P. Zoller, *Phys. Rev. Lett.* **78**, 390 (1997); I. L. Chuang and M. A. Nielsen, *J. Mod. Opt.* **44**, 2455 (1997); J. B. Altepeter *et al.*, *Phys. Rev. Lett.* **90**, 193601 (2003); F. De Martini, A. Mazzei, M. Ricci, and G. M. D'Ariano, *Phys. Rev. A* **67** 062307 (2003); J. L. O'Brien *et al.*, *quant-ph/0402166*.